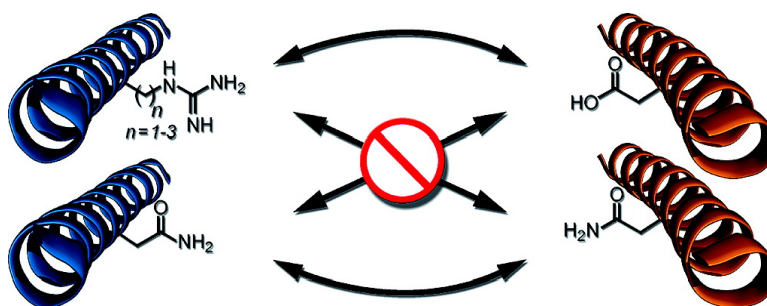


Orthogonal Recognition in Dimeric Coiled Coils via Buried Polar-Group Modulation

Maria L. Diss, and Alan J. Kennan

J. Am. Chem. Soc., **2008**, 130 (4), 1321-1327 • DOI: 10.1021/ja076265w

Downloaded from <http://pubs.acs.org> on February 8, 2009



More About This Article

Additional resources and features associated with this article are available within the HTML version:

- Supporting Information
- Links to the 3 articles that cite this article, as of the time of this article download
- Access to high resolution figures
- Links to articles and content related to this article
- Copyright permission to reproduce figures and/or text from this article

[View the Full Text HTML](#)

able glutamic acid/lysine (Glu/Lys) interactions, while avoiding presumably repulsive Glu/Glu or Lys/Lys pairings. Strategies for *a/d* control include alignment of sterically matched side chains or buried polar groups. This array of fundamental design work has facilitated applications in protein misfolding models,⁴ materials chemistry,⁵ and biotechnology.⁶

We have previously developed steric matching of hydrophobic core side chains as a route to specific trimer formation.⁷ Seeking to establish similar levels of control in dimeric systems, we have begun to explore new buried polar interactions. The most common use of buried polar contacts in dimeric coiled coils is to include a single core asparagine (Asn), which has been shown to impart structural uniqueness with respect to both oligomerization state and strand orientation, although other polar contacts have also been developed.⁸ Despite unquestionable utility, the Asn strategy is necessarily limited to a single recognition event. Considerably more self-assembly problems could be addressed if two independent parallel dimers could be

generated by simply mixing four different peptides. This demands new core recognition pairs, which can direct specific and stable dimer formation while ignoring the presence of alternative complexes.

In the course of other investigations, we have developed a convenient synthetic methodology for preparing guanidylated amino acid residues during solid-phase peptide synthesis.⁹ Here we report use of a slight modification to this method to prepare several peptides with a single core guanidylated side chain of varying length. A detailed evaluation of heterodimeric assemblies with guanidine/guanidine, guanidine/amide, or guanidine/carboxylic acid buried polar contacts reveals a large number of reasonably stable coiled coil dimers ($T_m \geq 60$ °C). Most significantly, three new combinations are demonstrated to function in the presence of an Asn/Asn driven dimerization.

Results and Discussion

As a starting sequence for investigating core interactions we focused on the Acid-p1/Base-p1 heterodimer designed by Kim and co-workers.¹⁰ Each strand of our parent dimer thus contains a leucine (Leu) core with a single Asn at position 14, and either Glu (pAsn_E) or Lys (pAsn_K) at each *e/g* location (Figure 1).¹¹ The other sequences differ in polar core residue identity, featuring guanidine or carboxylic acid side chains of varying length. In addition to arginine (Arg, three methylenes in the side chain), we employed guanidylated diaminopropionic acid (Dap*, one methylene) and diaminobutyric acid (Dab*, two methylenes). The acidic (pDap*_E, pDab*_E, pArg_E) and basic (pDap*_K, pDab*_K, pArg_K) versions of each sequence differ only in *e/g* substitution. We also investigated acidic peptides bearing aspartic acid (Asp) or Glu at the polar core position (pAsp_E, pGlu_E).

The sequences containing only natural side-chain structures were prepared via standard solid-phase methods using commercial amino acids. The requisite chain shortened Arg analogues were prepared using a modification of our previously reported on-resin guanidinylation method.¹²

With the peptides in hand, we began by investigating heterodimers bearing identical guanidine side chains in place of the parent asparagines (Figure 2). Although we anticipated that burial of like charges might substantially destabilize potential complexes, circular dichroism (CD) spectra of 1:1 pDab*_K/pDab*_E, and pArg_K/pArg_E mixtures exhibit dramatic helicity increases compared to the average component signals (Figure 2C/E).¹³ Thermal unfolding experiments reveal cooperative transitions only for the mixtures, which also have reasonably

- (3) (a) Tsurkan, M. V.; Ogawa, M. Y. *Inorg. Chem.* **2007**, *46*, 6849–6851. (b) Steinmetz, M. O.; Jelesarov, I.; Matousek, W. M.; Honnappa, S.; Jahnke, W.; Missimer, J. H.; Frank, S.; Alexandrescu, A. T.; Kammerer, R. A. *Proc. Nat. Acad. Sci. U.S.A.* **2007**, *104*, 7062–7067. (c) Shang, J.; Geva, E. *J. Phys. Chem. B* **2007**, *111*, 4178–4188. (d) Ryan, S. J.; Kennan, A. *J. Am. Chem. Soc.* **2007**, *129*, 10255–10260. (e) Portwich, M.; Keller, S.; Strauss, H. M.; Mahrenholz, C. C.; Kretzschmar, I.; Kramer, A.; Volkmer, R. *Angew. Chem., Int. Ed.* **2007**, *46*, 1654–1657. (f) Nikolaev, Y.; Pervushin, K. *J. Am. Chem. Soc.* **2007**, *129*, 6461–6469. (g) Yoder, N. C.; Kumar, K. *J. Am. Chem. Soc.* **2006**, *128*, 188–191. (h) Son, S.; Tanrikulu, C.; Tirrell, D. A. *ChemBioChem* **2006**, *7*, 1251–1257. (i) Meier, M.; Burkhard, P. *J. Struct. Biol.* **2006**, *155*, 116–129. (j) Mason, J. M.; Schmitz, M. A.; Mueller, K. M.; Arndt, K. M. *Proc. Nat. Acad. Sci. U.S.A.* **2006**, *103*, 8989–8994. (k) Liu, J.; Zheng, Q.; Deng, Y.; Cheng, C.-S.; Kallenbach, N. R.; Lu, M. *Proc. Nat. Acad. Sci. U.S.A.* **2006**, *103*, 15457–15462. (l) Lee, K.-H.; Cabello, C.; Hemmingsen, L.; Marsh, E. N. G.; Pecoraro, V. L. *Angew. Chem., Int. Ed.* **2006**, *45*, 2864–2868. (m) Hadley, E. B.; Gellman, S. H. *J. Am. Chem. Soc.* **2006**, *128*, 16444–16445. (n) Dong, H.; Hartgerink, J. D. *Biomacromolecules* **2006**, *7*, 691–695. (o) Bunagan, M. R.; Cristian, L.; DeGrado, W. F.; Gai, F. *Biochemistry* **2006**, *45*, 10981–10986. (p) Bjelic, S.; Karshikoff, A.; Jelesarov, I. *Biochemistry* **2006**, *45*, 8931–8939. (q) Balakrishnan, G.; Hu, Y.; Case, M. A.; Spiro, T. G. *J. Phys. Chem. B* **2006**, *110*, 19877–19883. (r) Acharya, A.; Rishi, V.; Vinson, C. *Biochemistry* **2006**, *45*, 11324–11332. (s) Yadav, M. K.; Redman, J. E.; Leman, L. J.; Alvarez-Gutierrez, J. M.; Zhang, Y.; Stout, C. D.; Ghadiri, M. R. *Biochemistry* **2005**, *44*, 9723–9732. (t) Sakurai, Y.; Mizuno, T.; Hiroaki, H.; Gohda, K.; Oku, J.-i.; Tanaka, T. *Angew. Chem., Int. Ed.* **2005**, *44*, 6180–6183. (u) Plecs, J. J.; Harbury, P. B.; Kim, P. S.; Alber, T. *J. Mol. Biol.* **2004**, *342*, 289–297. (v) Marti, D. N.; Bosshard, H. R. *Biochemistry* **2004**, *43*, 12436–12447. (w) Kwok, S. C.; Hodges, R. S. *J. Biol. Chem.* **2004**, *279*, 21576–21588. (x) Gurmon, D. G.; Whitaker, J. A.; Oakley, M. G. *J. Am. Chem. Soc.* **2003**, *125*, 7518–7519. (y) McClain, D. L.; Gurmon, D. G.; Oakley, M. G. *J. Mol. Biol.* **2002**, *324*, 257–270. (z) Vu, C.; Robblee, J.; Werner, K. M.; Fairman, R. *Protein Sci.* **2001**, *10*, 631–637.
- (4) (a) Dong, H.; Hartgerink, J. D. *Biomacromolecules* **2007**, *8*, 617–623. (b) Yadav, M. K.; Leman, L. J.; Price, D. J.; Brooks, C. L., III; Stout, C. D.; Ghadiri, M. R. *Biochemistry* **2006**, *45*, 4463–4473. (c) Pagel, K.; Wagner, S. C.; Samedov, K.; Von Berlepsch, H.; Boettcher, C.; Koksche, B. *J. Am. Chem. Soc.* **2006**, *128*, 2196–2197. (d) Ambroggio, X. I.; Kuhlman, B. *J. Am. Chem. Soc.* **2006**, *128*, 1154–1161. (e) Cerasoli, E.; Sharpe, B. K.; Woolfson, D. N. *J. Am. Chem. Soc.* **2005**, *127*, 15008–15009.
- (5) (a) Papapostolou, D.; Smith, A. M.; Atkins, E. D. T.; Oliver, S. J.; Ryadnov, M. G.; Serpell, L. C.; Woolfson, D. N. *Proc. Nat. Acad. Sci. U.S.A.* **2007**, *104*, 10853–10858. (b) Zimenkov, Y.; Dublin, S. N.; Ni, R.; Tu, R. S.; Breedveld, V.; Apkarian, R. P.; Conticello, V. P. *J. Am. Chem. Soc.* **2006**, *128*, 6770–6771. (c) Shen, W.; Zhang, K.; Kornfield, J. A.; Tirrell, D. A. *Nat. Mater.* **2006**, *5*, 153–158. (d) Raman, S.; Machaidze, G.; Lustig, A.; Aebi, U.; Burkhard, P. *Nanomedicine* **2006**, *2*, 95–102. (e) Kovacic, B. C.; Kokona, B.; Schwab, A. D.; Twomey, M. A.; De Paula, J. C.; Fairman, R. *J. Am. Chem. Soc.* **2006**, *128*, 4166–4167. (f) Farmer, R. S.; Argust, L. M.; Sharp, J. D.; Kiick, K. L. *Macromolecules* **2006**, *39*, 162–170.
- (6) (a) Mason, J. M.; Mueller, K. M.; Arndt, K. M. *Biochemistry* **2007**, *46*, 4804–4814. (b) Leman, L. J.; Weinberger, D. A.; Huang, Z.-Z.; Wilcoxon, K. M.; Ghadiri, M. R. *J. Am. Chem. Soc.* **2007**, *129*, 2959–2966. (c) Yuzawa, S.; Mizuno, T.; Tanaka, T. *Chem. Eur. J.* **2006**, *12*, 7345–7352. (d) Woolley, G. A.; Jaikaran, A. S. I.; Berezovski, M.; Calarco, J. P.; Krylov, S. N.; Smart, O. S.; Kumita, J. R. *Biochemistry* **2006**, *45*, 6075–6084. (e) Zhang, K.; Diehl, M. R.; Tirrell, D. A. *J. Am. Chem. Soc.* **2005**, *127*, 10136–10137. (f) Magliery, T. J.; Wilson, C. G. M.; Pan, W.; Mishler, D.; Ghosh, I.; Hamilton, A. D.; Regan, L. *J. Am. Chem. Soc.* **2005**, *127*, 146–157. (g) Zhou, M.; Ghosh, I. *Org. Lett.* **2004**, *6*, 3561–3564.
- (7) (a) Schnarr, N. A.; Kennan, A. J. *J. Org. Lett.* **2005**, *7*, 395–398. (b) Schnarr, N. A.; Kennan, A. J. *J. Am. Chem. Soc.* **2004**, *126*, 14447–14451.
- (8) (a) Straussman, R.; Ben-Ya'acov, A.; Woolfson, D. N.; Ravid, S. *J. Mol. Biol.* **2007**, *366*, 1232–1242. (b) Lear, J. D.; Gratkowski, H.; Adamian, L.; Liang, J.; DeGrado, W. F. *Biochemistry* **2003**, *42*, 6400–6407. (c) Schneider, J. P.; Kretsinger, J.; *J. Am. Chem. Soc.* **2003**, *125*, 7907. (d) Akey, D. L.; Malashkevich, V. N.; Kim, P. S. *Biochemistry* **2001**, *40*, 6352–6360. (e) Oakley, M. G.; Kim, P. S. *Biochemistry* **1998**, *37*, 12603–12610. (f) Zeng, X.; Herndon, A. M.; Hu, J. C. *Proc. Natl. Acad. Sci. U.S.A.* **1997**, *94*, 3673–3678. (g) Schneider, J. P.; Lear, J. D.; DeGrado, W. F. *J. Am. Chem. Soc.* **1997**, *119*, 5742. (h) Gonzalez, L., Jr.; Woolfson, D. N.; Alber, T. *Nat. Struct. Biol.* **1996**, *3*, 1011–1018. (i) Lumb, K. J.; Kim, P. S. *Biochemistry* **1995**, *34*, 8642–8.
- (9) Zhang, Y.; Kennan, A. J. *J. Org. Lett.* **2001**, *3*, 2341–2344. See Supporting Information for details.
- (10) O'Shea, E. K.; Lumb, K.; Kim, P. S. *Curr. Biol.* **1993**, *3*, 658–667.
- (11) These two peptides are not technically the same as Acid-p1/Base-p1, only because they differ in the chosen spectroscopic label (tryptophan versus acetamidobenzoyl). To avoid confusion they are given names consistent with the nomenclature scheme of the other sequences.
- (12) See Supporting Information for details.
- (13) See Supporting Information for similar plots involving all other heterodimers examined in this work.

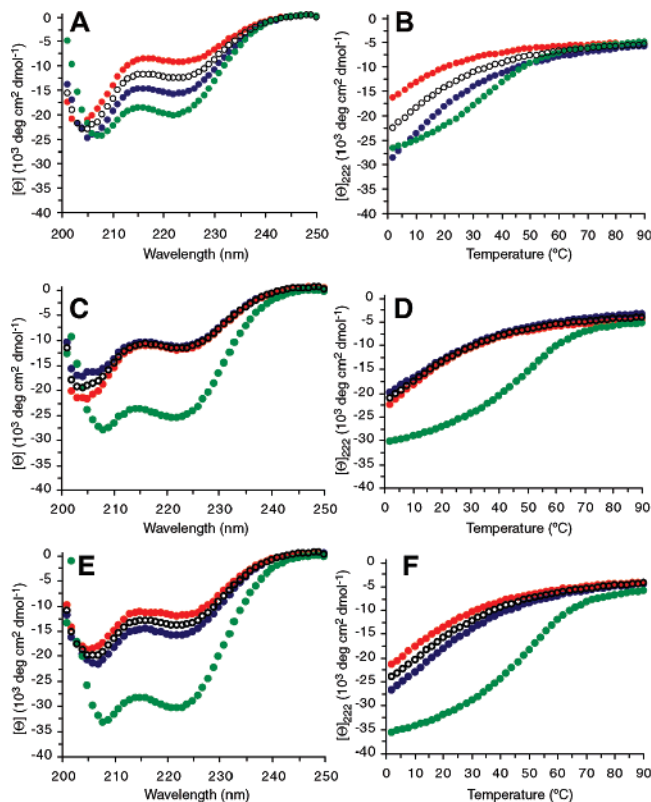


Figure 2. Buried guanidine–guanidine interactions. Wavelength (A, C, E) and thermal denaturation (B, D, F) CD spectra for pure solutions of pXaa_K (red) and pXaa_E (blue), where Xaa = Dap* (A, B), Dab* (C, D), and Arg (E, F). In each case, traces for an equimolar mixture (green) and the calculated weighted-average signal (open circles) are also given.¹⁷

high stability (Figure 2D/F, $T_m = 59$ °C in each case), albeit diminished from the parent pAsn_E/pAsn_K complex ($T_m = 77$ °C). Both observations point to a specific and significant interaction between the component peptides, consistent with heterodimer formation. The pDap_K/pDap_E mixture displays a more subtle but similar effect, supporting an overall trend of increased heterodimer stability with increases in side-chain length (Figure 2A/B).

The observation of an Arg/Arg contact that is only somewhat destabilizing compared to an Asn/Asn interaction is consistent with some contact potential estimates derived from statistical analyses of protein structures.¹⁴ One such method predicts contact energies of -1.68 and -1.55 kcal/mol for Asn/Asn and Arg/Arg, respectively.^{14b} Both are significantly less stabilizing than Leu/Leu, Ile/Ile, or Val/Val contacts (-7.37 , -6.54 , -5.52 kcal/mol, respectively), consistent with increased T_m values for coiled coils with purely hydrophobic cores (which nonetheless typically form nonspecific complexes).

Having observed reasonable stability in complexes which pair identical guanidine side chains, we deemed it worthwhile to examine the analogous mixed-core systems. Spectra of equimolar pDap*_K/pDab*_E, pDap*_K/pArg_E, and pDab*_K/pArg_E mixtures also exhibit reasonable room-temperature helicities and cooperative thermal unfolding profiles (Figure 3, Table 1). A subtle but noticeable stability trend again favors those complexes with more total methylenes in the buried polar side chains.

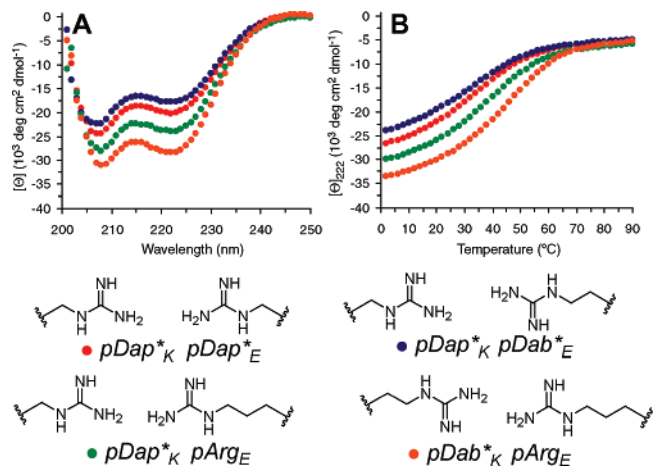


Figure 3. Mixed guanidine–guanidine interactions. Wavelength (A) and thermal denaturation (B) CD spectra for the indicated equimolar mixtures.¹⁷

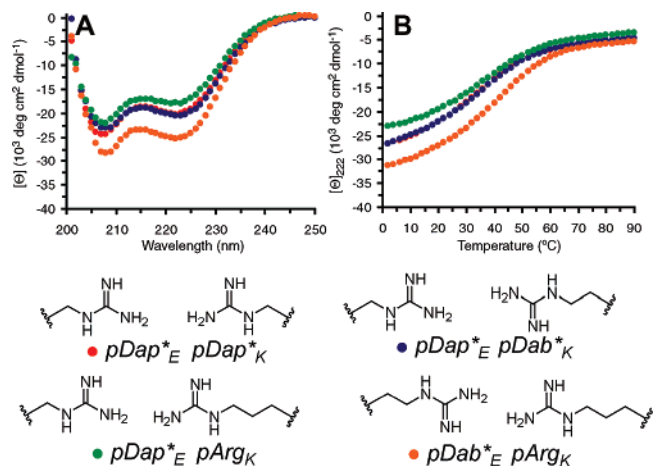


Figure 4. Core-swapped mixed guanidine–guanidine interactions. Wavelength (A) and thermal denaturation (B) CD spectra for the indicated equimolar mixtures.¹⁷

Table 1. Observed T_m Values for Guanidine Core Pairs

sample	T_m (°C)	sample	T_m (°C)
pDap* _K /pDap* _E	49	pDap* _K /pArg _E	47
pDab* _K /pDab* _E	59	pDab* _K /pArg _E	55
pArg _K /pArg _E	59	pDap* _E /pArg _K	47
pDap* _K /pDab* _E	43	pDab* _E /pArg _K	51
pDap* _E /pDab* _K	49		

Mixed-core complexes introduce another possible complication, since exchanging the polar core residues on the acidic and basic strands produces a distinct complex (e.g., pDap*_K/pDab*_E is not the same as pDap*_E/pDab*_K). Although we expected any differences to be minimal, we nonetheless examined the reverse mixed-core mixtures pDap*_E/pDab*_K, pDap*_E/pArg_K, and pDab*_E/pArg_K (Figure 4, Table 1). Somewhat surprisingly, a modest compression in stability range was observed, such that the two mixed pDap*_E complexes are very similar to each other and to the original pDap*_K/pDap*_E mixture. Even the pDab*_E/pArg_K signal is closer to the others than its counterpart is. Though observable, the differences were small enough that we hesitate to apply detailed structural rationales.

Having discovered surprisingly stable complexes with electrostatically repulsive guanidine/guanidine pairings, we next examined the interaction of each guanidinylated side chain with the parent neutral Asn residue, expecting a further increase in

(14) (a) Gromiha, M. M.; Selvaraj, S. *Prog. Biophys. Mol. Biol.* **2004**, *86*, 235–277. (b) Miyazawa, S.; Jernigan, R. L. *J. Mol. Biol.* **1996**, *256*, 623–644. (c) For a discussion of potential difficulties with such analyses see: Thomas, P. D.; Dill, K. A. *J. Mol. Biol.* **1996**, *257*, 457–489.

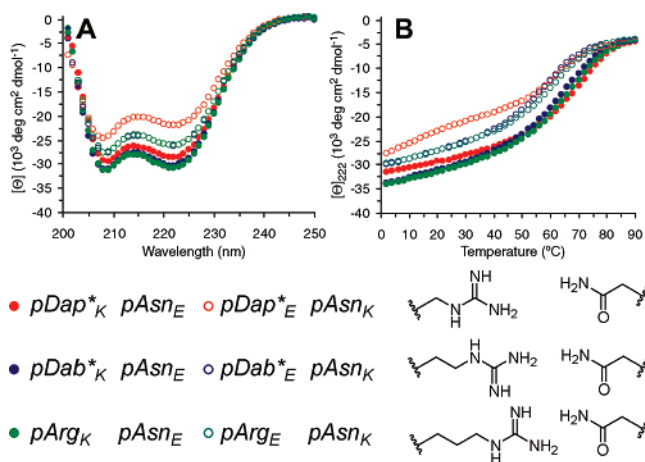


Figure 5. Guanidine/Asn core interactions. Wavelength (A) and thermal denaturation (B) CD spectra for the indicated equimolar mixtures.¹⁷ Closed and open circles of the same color indicate data from complexes that differ by exchange of the indicated buried polar side chains (from the acidic or basic peptide to the other).

Table 2. Observed T_m Values for Guanidine Amide/acid Core Pairs

sample	T_m (°C)	sample	T_m (°C)
$pDap^*_K/pAsn_E$	73	$pDap^*_K/pAsp_E$	61
$pDab^*_K/pAsn_E$	71	$pDab^*_K/pAsp_E$	67
$pArg_K/pAsn_E$	71	$pArg_K/pAsp_E$	65
$pDap^*_E/pAsn_K$	63	$pDap^*_K/pGlu_E$	59
$pDab^*_E/pAsn_K$	63	$pDab^*_K/pGlu_E$	63
$pArg_E/pAsn_K$	65	$pArg_K/pGlu_E$	63

overall stability. Examination of wavelength and thermal unfolding CD data support this expectation (Figure 5, Table 2). Equimolar mixtures of $pDap^*_K$, $pDab^*_K$, and $pArg_K$ with $pAsn_E$ exhibited cooperative unfolding transitions and substantial melting temperatures ($T_m = 71–73$ °C). To determine the impact of local strand interactions, the reverse complexes, formed by mixing $pDap^*_E$, $pDab^*_E$, and $pArg_E$ with $pAsn_K$, were also investigated (Figure 5, Table 2). As with the mixed guanidine complexes, a small but definite stability distinction exists, favoring those with guanidylated side chains on the basic peptide (e.g., $T_m = 71$ °C for $pArg_K/pAsn_E$, versus 65 °C for $pArg_E/pAsn_K$). The difference is particularly pronounced in the room-temperature helicity of the two Dap^* complexes, although the gap narrows at the melting transition. Overall, a reduced stability variance is observed within each set, meaning that length of the guanidine side chain seems largely irrelevant when paired opposite Asn, as opposed to another guanidine.

The final set of interactions examined mix each guanidine side chain with Asp or Glu residues, resulting in an overall neutral complex which may benefit from core electrostatic attraction. As with other the other core pairings, equimolar mixtures of $pDap^*_K$, $pDab^*_K$, and $pArg_K$ with either $pAsp_E$ or $pGlu_E$ exhibit good helicities and thermal stabilities. (Figure 6–7, Table 2). The range of T_m values (59 to 67 °C) is comparable to those of the guanidine/amide pairs, albeit slightly lower. The guanidine/acid pairs also display a similar insensitivity to polar residue chain length, with only a small change between the $pDap^*_K/pAsp_E$ and $pArg_K/pGlu_E$ complexes.

With a now substantial array of feasible heterodimers available, we began to explore prospects for new orthogonal recognition pairs. A comparison of melting curves for each

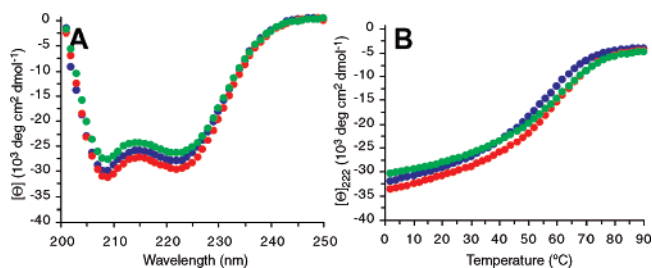


Figure 6. Guanidine/Asp core interactions. Wavelength (A) and thermal denaturation (B) CD spectra for equimolar mixtures of $pAsp_E$ with $pDap^*_K$ (blue), $pDab^*_K$ (red), and $pArg_K$ (green).¹⁷

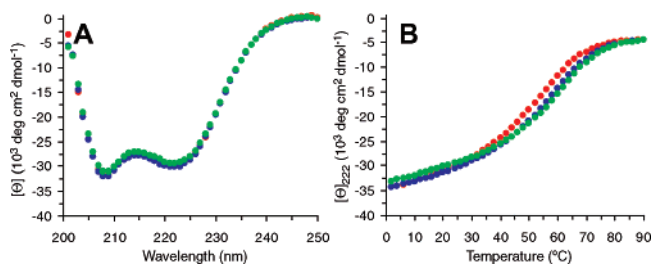


Figure 7. Guanidine/Glu core interactions. Wavelength (A) and thermal denaturation (B) CD spectra for equimolar mixtures of $pGlu_E$ with $pDap^*_K$ (red), $pDab^*_K$ (blue), and $pArg_K$ (green).¹⁷

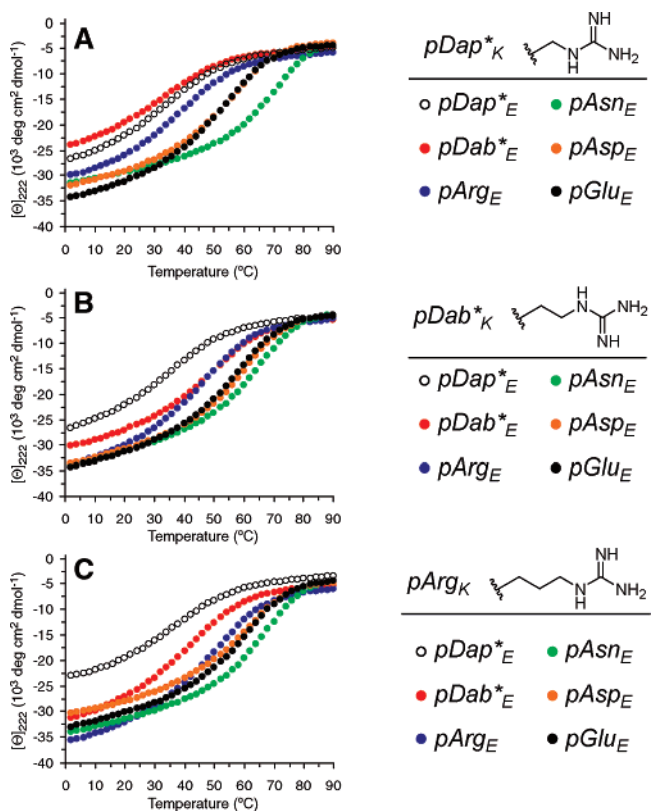


Figure 8. Melting curve comparisons. Thermal unfolding data for equimolar solutions of $pDap^*_K$ (A), $pDab^*_K$ (B), and $pArg_K$ (C) with each of the indicated acidic peptides replotted for comparison.¹⁷

guanidine side chain paired with each of its partners reveals some interesting features (Figure 8). In each case, solutions with $pAsn_E$ as the partner core residue exhibit the most stable profiles, followed by the $pAsp_E$ and $pGlu_E$ complexes, and finally the various guanidine/guanidine mixtures. The degree of separation between these classes varies quite significantly, with sharp distinctions drawn for interactions with $pDap^*_K$, and a gradual

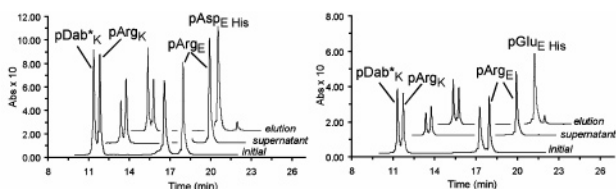


Figure 9. Ni-NTA analysis of pArgE/pArgK pDab*_K Asp/Glu selective dimer formation. Equimolar initial mixtures of pArg_K/pArg_E/pDab*_K/pAsp_E His (left) and pArg_K/pArg_E/pDab*_K/pGlu_E His (right) give rise to supernatant and elution fractions containing all reasonable complexes. Initial solutions are 20 μM total peptide, pH 7.0, 150 mM NaCl, 10 mM phosphate.

blurring of those distinctions in moving to the longer side chains. At the extreme, the trace for pArg_K/pArg_E is not that different from those of the pAsp_E and pGlu_E mixtures (Figure 8C).

The reasonable stability of the Arg/Arg core pair led us to examine it as an initial candidate for an interaction which could be preserved in the presence of another heterodimer. Similarly, the complexes with Dab*/Asp and Dab*/Glu pairs demonstrated reasonable melting temperatures and were chosen as the alternate partners. Thus it was hoped that equimolar mixtures of pArg_K/pArg_E/pDab*_K/pAsp_E and pArg_K/pArg_E/pDab*_K/pGlu_E would each afford two separate dimers, rather than a mixture of the four energetically reasonable assemblies (discounting electrostatically incompatible binding of two acidic or basic peptides).

To assay for dimer specificity, we employed a Ni-NTA affinity method we have previously used extensively to measure coiled-coil stoichiometries.^{7,12} An N-terminal GlyGly(His)₆ tag confers affinity for Ni-NTA agarose beads upon both the tagged peptide and any species which binds to it. After exposure to beads, removal of the supernatant, washing to eliminate low-affinity peptides, and elution with imidazole buffer to recover bound material, each fraction is analyzed by HPLC. In the present case, if one of the four peptides is tagged and orthogonal recognition is operative, one expects the tagged peptide and its partner to dominate the elution fraction, while the two matched untagged peptides reside in the supernatant.

For the initial two mixtures, tagged derivatives of the Asp (pAsp_E His) and Glu (pGlu_E His) peptides were synthesized using standard methods. Unfortunately, analysis of each mixture demonstrates essentially nonspecific recognition (Figure 9). Both elution fractions contain each of the basic peptides, suggesting that pArg_K/pAsp_E and pArg_K/pGlu_E complexes form in addition to the desired ones. The supernatants also contain both basic species, consistent with formation of the unintended pDab*_K/pArg_E complex in each case.

Following this lack of success using two new core–core matchups, we next investigated whether guanidine/guanidine peptides could recognize each other in the context of the known Asn/Asn interaction, which would require identifying only one new viable core–core interaction. Thus equimolar solutions of pAsn_K/pAsn_E/pDap*_K/pDap*_E, pAsn_K/pAsn_E/pDab*_K/pDab*_E, and pAsn_K/pAsn_E/pArg_K/pArg_E were analyzed by Ni-NTA affinity (the basic Asn peptide was His tagged in each case). Once again, essentially no specificity was observed, as both supernatant and elution fractions contained significant quantities of each acidic peptide in all three experiments.¹²

In light of these results we began to consider that selection of two reasonable complexes was not a sufficient criterion to ensure specific recognition. In particular, we examined stabilities of the alternative complexes as an additional consideration to

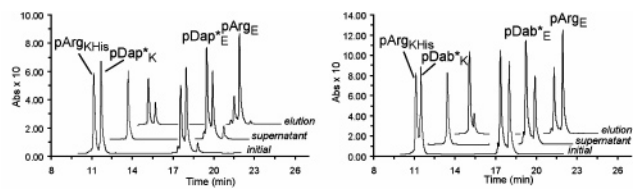


Figure 10. Ni-NTA analysis of Arg/Arg, Dap*/Dap* and Dab*/Dab* complexes. Equimolar mixtures of pArg_K/pArg_E/pDap*_K/pDap*_E His (left) and pArg_K/pArg_E/pDab*_K/pDab*_E His (right) give rise to supernatant and elution fractions containing all reasonable complexes. Solutions are as in Figure 9.

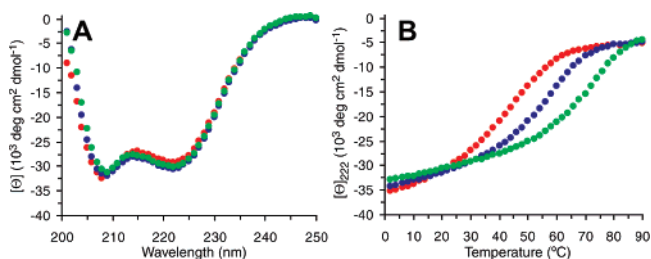


Figure 11. Asn/acid interactions. Wavelength (A) and thermal denaturation (B) CD spectra for equimolar mixtures of pAsn_K/pAsn_E (green), pAsn_K/pGlu_E (blue), and pAsn_K/pAsp_E (red).¹⁷

Table 3. Observed T_m Values for Asn/acid Core Pairs

sample	T_m (°C)	sample	T_m (°C)
pAsn _K /pAsp _E	51	pAsn _K /pAsn _E	77
pAsn _K /pGlu _E	65		

predict likely candidates. By this measure, our initial efforts seemed less promising. Using melting temperatures as a crude measure of stability, we recognized that the reasonable pArg_K/pArg_E interaction could be balanced by the comparable pDab*_K/pArg_E (or pDab*_K/pGlu_E) affinity. Similarly, the very stable pAsn_K/pAsn_E contact ($T_m = 77$ °C) is nearly balanced by the uniformly high guanidine/amide T_m values (more than balanced for the relatively weak pDab*_K/pDab*_E interaction).

With this view in mind, we next targeted all-guanidine systems. Mixtures of pDap*_K with pDap*_E or pArg_E exhibited similar stabilities ($T_m = 49$ and 47 °C, respectively), while pArg_K demonstrated a preference for pArg_E over pDap*_E ($T_m = 59$ vs 47 °C). Similar arguments apply to pDab*_K, with slightly more favorable numbers (T_m values of 59 vs 51 °C and 59 vs 55 °C). Despite this determination, analysis of equimolar pArg_K/pArg_E/pDap*_K/pDap*_E, and pArg_K/pArg_E/pDab*_K/pDab*_E mixtures (using pArg_K His) again failed to support high levels of specificity (Figure 10). However, some relative preference was observed (indicated by slightly unequal ratios of the acidic peptides in supernatant and elution fractions). We therefore sought to extend this approach to even more unbalanced pairs.

Using the reasoning above, selective recognition seems most likely when at least one of the unintended complexes is destabilized. Thus to exploit the stable Asn/Asn contact we sought another pair in which at least one partner is mismatched with Asn. Although the guanidine/Asn contacts were largely favorable, we wondered if the same would apply to Asp or Glu matched with Asn. Accordingly, we measured wavelength and thermal unfolding CD profiles for equimolar solutions of pAsn_K/pAsp_E and pAsn_K/pGlu_E, and compared them with the parent pAsn_K/pAsn_E complex (Figure 11, Table 3).

Encouragingly, Asp appears to be relatively mismatched with Asn ($T_m = 51$ °C). In contrast, the interaction with Glu seems

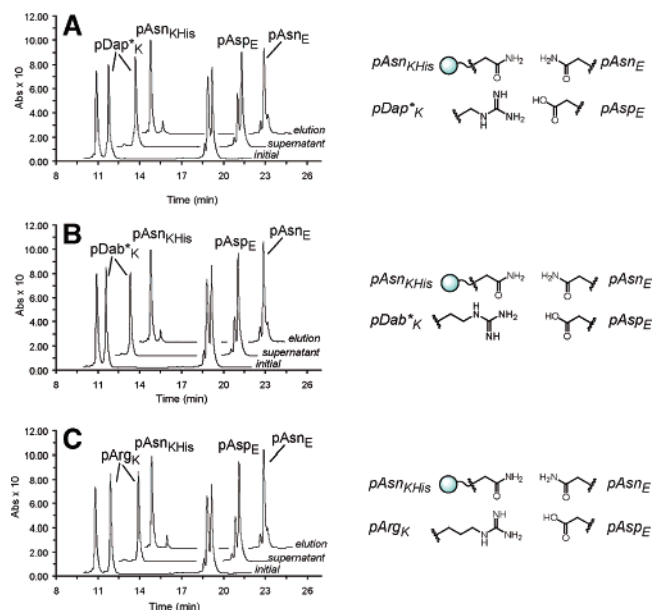


Figure 12. Ni-NTA analysis of four component Asn/Asn and Gdn/Asp mixtures. Equimolar ratios of (A) pAsn_{KHis}/pAsn_E/pDap*_K/pAsp_E, (B) pAsn_{KHis}/pAsn_E/pDab*_K/pAsp_E, and (C) pAsn_{KHis}/pAsn_E/pArg_K/pAsp_E all demonstrate specific recognition. Elution fractions and supernatants are dominated by the Asn peptides, indicating preferential binding of pAsp_E. Solutions are as in Figure 9.

relatively strong ($T_m = 65$ °C). Thus we predicted that guanidine/Asp peptides should be able to specifically recognize each other in the presence of the Asn/Asn contact, while the corresponding guanidine/Glu complexes would be nonspecific. To examine both of these possibilities, equimolar solutions of pAsn_K/pAsn_E with pDap*_K/pAsp_E, pDab*_K/pAsp_E, pArg_K/pAsp_E, pDap*_K/pGlu_E, pDab*_K/pGlu_E, and pArg_K/pGlu_E were investigated by Ni-NTA methods (using pAsn_{KHis} in all but the latter case, which used pGlu_{EHis}).

Analysis of the Asp complexes reveals that indeed these pairs are capable of orthogonal recognition in the presence of an Asn/Asn interaction (Figure 12). In each case, the elution fraction is dominated by pAsn_{KHis} and pAsn_E, while the supernatant contains largely the guanidine/Asp peptides. To our knowledge this is the first example of simultaneous self-selection of independent heterodimeric coiled coils driven only by a single-residue buried polar-residue substitution.

Further supporting the exquisite specificity of this interaction, the corresponding guanidine/Glu complexes, differing only by the addition of a single methylene unit in the core, do not display correspondingly specific binding (Figure 13). In each case, as with the early experiments, significant quantities of each possible complex is indicated by the presence of additional peptides in both supernatant and elution fractions.

The apparent success of guanidine/Asp complexes in specific orthogonal recognition led us to further characterize each heterodimer. Support for dimer formation and stoichiometry was obtained by Ni-NTA experiments. When equimolar mixtures of pDap*_K, pDab*_K, and pArg_K with a His-tagged pAsp_E derivative are exposed to Ni-NTA agarose beads, the elution fractions in each case contain one equivalent of each peptide (Figure 14).

Sedimentation equilibrium analytical ultracentrifugation results are also consistent with dimer formation. Equimolar solutions of pDap*_K/pAsp_E ($M_{r, \text{calcd}} = 7200$, $M_{r, \text{obs}} = 7543$),

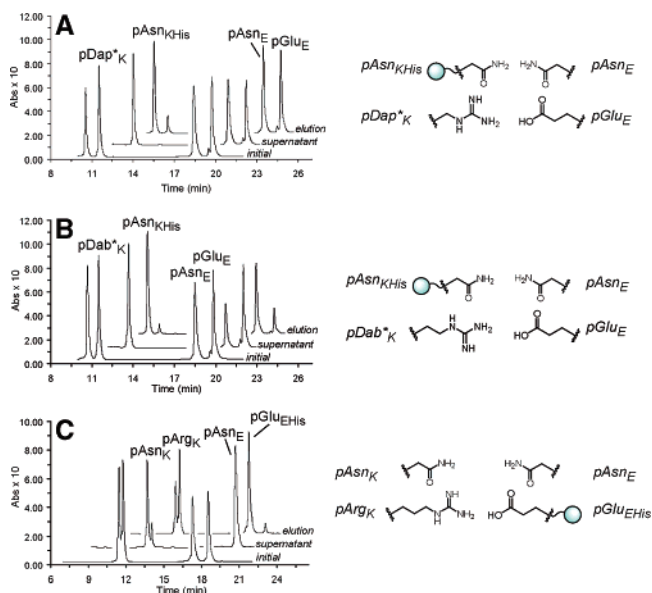


Figure 13. Ni-NTA analysis of four component Asn/Asn and Gdn/Glu mixtures. Equimolar ratios of (A) pAsn_{KHis}/pAsn_E/pDap*_K/pGlu_E, (B) pAsn_{KHis}/pAsn_E/pDab*_K/pGlu_E, and (C) pAsn_{KHis}/pAsn_E/pArg_K/pGlu_{EHis} all demonstrate nonspecific recognition. Elution fractions and supernatants are consistent with formation of all possible dimers in significant quantities. Solutions are as in Figure 9.

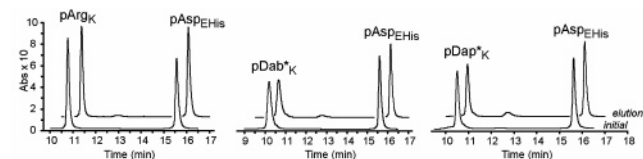


Figure 14. Ni-NTA analysis of Gdn/Asp heterodimers. In all three cases, one equivalent of the guanidylated peptide is retained in the elution fraction, starting from equimolar mixtures. Solutions are as in Figure 9, except that initial concentrations are 10 μ M total peptide.

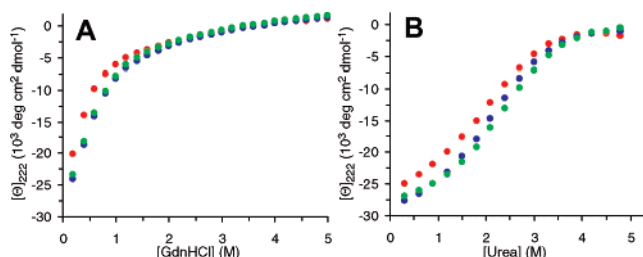


Figure 15. GdnHCl (A) and urea (B) denaturation data for equimolar mixtures of pAsp_E with pDap*_K (red), pDab*_K (blue), and pArg_K (green). Solutions are as in Figure 9.

pDab*_K/pAsp_E ($M_{r, \text{calcd}} = 7214$, $M_{r, \text{obs}} = 7589$), and pArg*_K/pAsp_E ($M_{r, \text{calcd}} = 7228$, $M_{r, \text{obs}} = 7634$) all gave apparent molecular weights within six percent of the calculated ones.¹⁵

Finally, we subjected each guanidine/Asp complex to chemical denaturation experiments (Figure 15). Although use of GdnHCl gave transitions with limited cooperativity, we speculated that ionic interactions could be important for such highly charged species.¹⁶ Accordingly, the experiments were repeated using urea unfolding, and the expected cooperative curves were observed. In addition to characterizing the Gdn/Asp dimers, we

(15) $M_{r, \text{obs}}$ values for pDap*_K and pDab*_K were obtained by assigning the unnatural amino acid a partial specific volume equal to the average value of all proteinogenic side chains. Substitution with either maximal or minimal values had little effect. See Supporting Information for details.

conducted Ni-NTA, centrifugation, and unfolding experiments on many of the other heterodimers reported here.¹²

To further quantify buried core interactions we considered a double-mutant cycle analysis, but selection of a usable reference state proved problematic. The standard Ala–Ala contact is unsuitable, as that substitution in the required core position dramatically alters oligomerization preferences in similar systems (a failing likely exhibited by other hydrophobic options).⁸ⁱ Polar groups capable of specifying oligomerization state would in turn presumably exhibit measurable new interactions in the single-mutant complexes.

Conclusions

The work described above establishes a surprisingly broad array of reasonably stable coiled-coil heterodimers with an assortment of buried polar interactions. Although dimers with neutral core pairings are more stable, the gap was smaller than expected, particularly for cores with two buried guanidines. Intriguing chain-length effects are observed, with the short-chain

Dap* residue exhibiting much more selective binding preferences than arginine in the same environment. Despite the overall relative tolerance of varying core residue chain length and charge states, only a select subset of these new heterodimers were capable of recognition based only on polar core residue identity. The outcomes of these experiments suggest that specific formation of two independent heterodimers from initial four-peptide mixtures requires that at least one of the alternative complexes must be mismatched. Thus poor stability of Asn/Asp cores is capable of directing impressive recognition levels. The lessons learned here provide a scaffold for future design of even more complicated and selective assemblies, which will expand further the already extensive applications of coiled coils in biotechnology and materials chemistry.

Acknowledgment. This work was supported by an NSF CAREER award to A.J.K. (Grant CHE-0239275).

Supporting Information Available: Detailed experimental procedures, descriptions of guanidinylation chemistry, additional CD, Ni-NTA, and analytical ultracentrifugation data. This material is available free of charge via the Internet at <http://pubs.acs.org>.

JA076265W

- (16) (a) Schellman, J. A. *Quart. Rev. Biophys.* **2005**, *38*, 351–361. (b) Schellman, J. A. *Biophys. Chem.* **2002**, *96*, 91–101. (c) Monera, O. D.; Kay, C. M.; Hodges, R. S. *Protein Sci.* **1994**, *3*, 1984–91. (d) Tanford, C. *Adv. Protein Chem.* **1970**, *24*, 1–95. (e) Robinson, D. R.; Jencks, W. P. *J. Am. Chem. Soc.* **1965**, *87*, 2462–70.
- (17) All wavelength spectra were recorded at 25°C, and solutions for all CD experiments contained 10 μ M total peptide in PBS buffer (150 mM NaCl, 10 mM phosphate, pH 7.0).